Laboratory Study of Hall Reconnection in Partially Ionized Plasmas

Eric E. Lawrence, Hantao Ji, Masaaki Yamada, and Jongsoo Yoo

Phys. Rev. Lett. **110**, 015001 — Published 2 January 2013

DOI: 10.1103/PhysRevLett.110.015001

Laboratory Study of Hall Reconnection in Partially Ionized Plasmas

Eric E. Lawrence, Hantao Ji, Masaaki Yamada, and Jongsoo Yoo

Princeton Plasma Physics Laboratory

Abstract

The effects of partial ionization ($n_i/n_n \lesssim 1\%$) on magnetic reconnection in the Hall regime have been studied systematically in the Magnetic Reconnection Experiment (MRX). It is shown that, when neutrals are added the Hall quadrupole field pattern and thus electron flow is unchanged while the ion outflow speed is reduced due to ion-neutral drag. However, in contrast to theoretical predictions, the ion diffusion layer width does not change appreciably. Therefore, the total ion outflow flux and the normalized reconnection rate are reduced.

PACS numbers: 52.30.Ex, 52.35.Vd, 52.25.Ya

Magnetic reconnection is a fundamental process in many naturally occurring and man-made magnetized plasmas. However, these plasmas are often weakly ionized: the lower solar atmosphere, protostellar and protoplanetary disks, galactic molecular clouds, and tokamak edge plasmas can have typical ionization fractions of 0.1–1% or lower. Reconnection is of particular importance in the solar atmosphere, as it is thought to be a trigger and/or a driver for eruptive events that originate in the weakly ionized photosphere and chromosphere [1], but couple to the hot, fully ionized corona [2]. The effects of weak ionization are often neglected, but can sometimes be modeled as single fluid with a modified resistivity or diffusion [3–5]. These models depend on the ion-neutral collisional mean free path being shorter than all relevant length scales. However, reconnection can have a large range of scales, so this approximation may not always be valid. For instance, coronal observations [6] have shown that reconnection features can break down into plasmoids [7, 8] that are much smaller than the overall system size. NASA's soon to be launched Interface Region Imaging Spectrograph (IRIS) mission [9] will return highly detailed observations of these regions, so an understanding of how reconnection works in partially ionized plasmas is of timely importance. While the smallest of these scales may still be beyond what is currently observable, an understanding of the underlying physics is vital for interpreting and benchmarking the simulation models used to analyze the observations.

Collisions with neutrals can have a number of important effects on the reconnection dynamics. Elastic electron-neutral collisions increase the plasma resistivity, which is ultimately how the change in magnetic topology occurs, at least in collisional plasmas. The effects of ion-neutral collisions are more subtle. Because of the comparable particle masses, a very strong ion-neutral drag force will act like static friction, and they will behave as a single fluid with an effective mass equal to the total mass density, $\rho = \rho_n + \rho_i$. Swanson *et al.* [10] previously observed this effect for hydromagnetic Alfvén waves. A recent theoretical study [11, 12] treated reconnection in partially ionized plasmas and found a similar result. In particular, the Alfvén speed,, $v_A = B/\sqrt{4\pi\rho_i}$, and ion inertial length, $\delta_i = \sqrt{c^2 m_i^2/4\pi\rho_i e^2}$, are modified to use ρ instead of ρ_i, or some fraction of ρ if the coupling is moderate. The ion inertial length is especially relevant to fast, Hall-mediated reconnection, as it sets the length scale on which such reconnection can occur [13]. This model is of particular interest since it uses a multi-fluid approach where ion and neutral dynamics are treated separately, instead of relying on a single fluid Pedersen/Cowling resistivity or ambipolar diffusion.

In this Letter, we present the first study of the effects of partial ionization on Hall reconnection

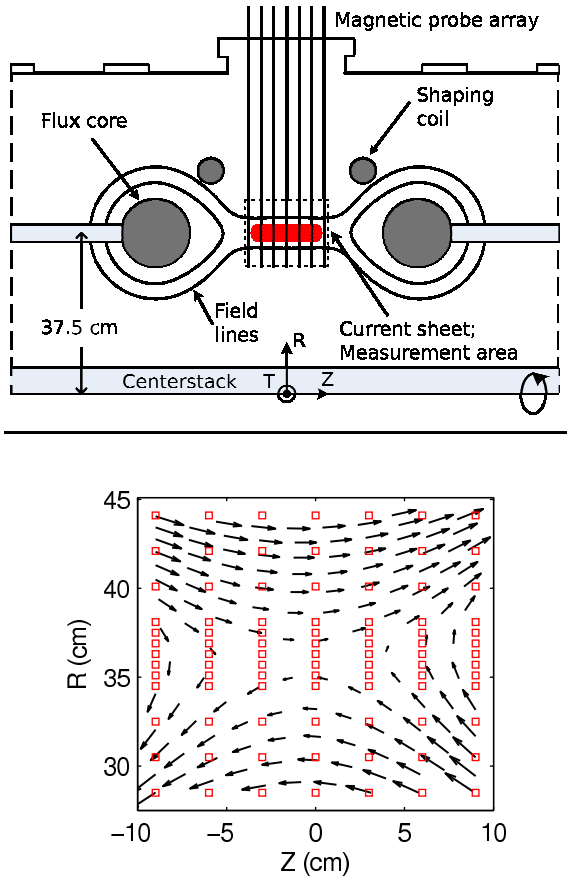

FIG. 1. (color online). (top) Experimental schematic near the reconnection region. Plasma and X-point magnetic field is produced by windings in the flux cores. Reconnection current sheet is diagnosed using an array of magnetic field coils. (bottom) Sample in-plane magnetic field vectors on an interpolated grid. Red squares show actual measurement locations.

in a laboratory plasma. Starting with conditions where neutral effects are nearly unimportant as a base case, we decrease the ionization level while keeping the plasma parameters fixed. We find that the outflow speed is reduced as previously predicted [11], but we do not observe corresponding changes in the ion layer scale size. Nonetheless, we find these observations to be consistent with the observed reconnection rate scaling, and discuss possible reasons for the discrepancies with the model.

These experiments were performed at the Magnetic Reconnection Experiment (MRX) facility [14]. A cross-sectional schematic of the cylindrical device near the reconnection region is shown in Fig. 1. The large gray circles represent the two toroidally-shaped flux cores. Each flux core contains two sets of windings: one set (PF) produces the initial X-point geometry, while the other (TF) produces the inductive electric field that breaks down the pre-filled working gas (helium in

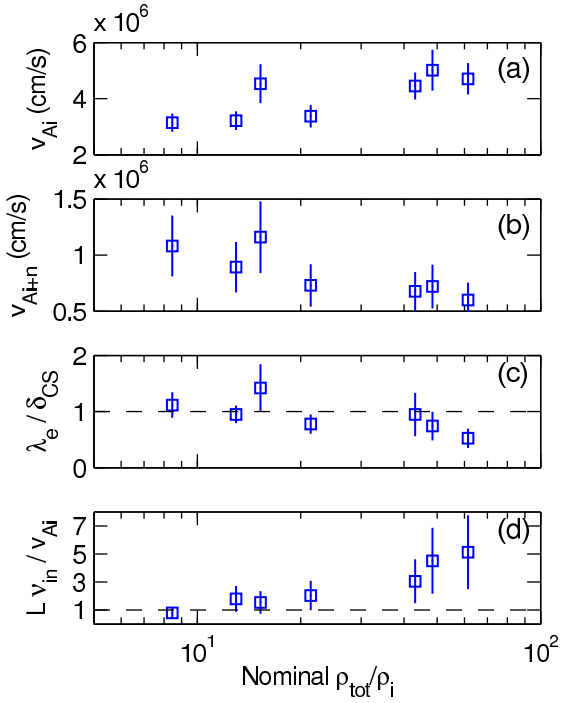

FIG. 2. (color online). Plasma parameters as a function of the nominal neutral density ratio, averaged over the quasi-steady period: (a) plasma Alfvén speed; (b) bulk (ion and neutral) Alfvén speed; (c) electron mean free path scaled to the current sheet width; (d) ion outflow time L/v_{Ai} scaled to ν_{in}.

these experiments). These experiments are performed in the "pull" reconnection regime, where the plasma is produced while PF current is decreasing and magnetic field lines are pulled towards the flux cores. This produces quasi-steady reconnection which lasts for ∼40 μs (∼$12\tau_A$). In this geometry, plasma and field lines flow into the reconnection region along the R direction, and outflows are in the Z direction. The current sheet is then in the toroidal (T) direction.

A 245-channel magnetic coil array measures all three components of the magnetic field in one RZ plane. The 20 cm × 16 cm measurement area is shown as a dashed box in Fig. 1a. A typical interpolated magnetic vector plot is shown in Fig. 1b, along with the positions of the actual coil locations. Radial resolution varies from 0.6–2.0 cm, which allows for detailed measurements across the current sheet, while the Z resolution is 3 cm. Assuming toroidal symmetry ($\partial/\partial T = 0$), we can compute poloidal flux ($\phi = \int B_Z dR$) and the reconnection electric field ($E_T = -(d\phi/dt)/2\pi R$).

Plasma density, electron temperature, and axial ion flow are measured at single points using standard triple Langmuir and Mach probe diagnostics [15]. An additional set of coils (shaping or SF; small gray circles) is pulsed during the pull reconnection phase, which injects axial magnetic

flux that uniformly drives the current sheet radially inward [16]. By tracking the radial location where $B_Z = 0$ as a function of time, we can reconstruct radial profile measurements without resorting to using multiple electrostatic probes that could perturb the plasma. Radial extents of 3-6 cm can generally be measured during the quasi-steady reconnection period.

The neutral density is primarily adjusted by changing the initial gas fill pressure, which is measured using a Baratron capacitance manometer. The pre-discharge neutral density can then be determined by assuming the gas to be an ideal gas at room temperature. Spectroscopic measurements of the 447.1 nm He I line and a collisional-radiative model [17] were used to estimate the neutral density inside the plasma during the discharge. These measurements were found to match the initial fill density within $\pm 50\%$ error bars. For the results presented here, we will take the initial fill pressure as the nominal neutral density value, and use these error bars where appropriate.

In this set of experiments, the helium fill pressure was varied from 5.5 to 45 mTorr ($n_n = 0.17$–1.4×10^{15} cm^{-3}). General plasma parameters are shown in Fig. 2. The TF coil currents and timing were adjusted to keep plasma density and temperature similar across the scan ($n_e \sim 2 \times 10^{13}$ cm^{-3} and $T_e \sim 6$ eV). The PF and SF coil currents and timing were kept constant in order to produce similar magnetic geometries. The plasma Alfvén speed, $v_{Ai} = B_0/\sqrt{4\pi\rho_i}$, calculated using the upstream reconnecting field B_0 and ion density at the current sheet center, increases slightly as neutrals are added (Fig. 2a). This is primarily due to increasing current density as ρ/ρ_i increases. The bulk Alfvén speed, v_{Ai+n}, calculated using the total ion and neutral mass density, is shown in Fig. 2b. Despite the increase in v_{Ai}, the increasing neutral density leads to a decreasing v_{Ai+n} in the scan. The electron gyrofrequency is $\sim 3 \times 10^9$ rad/s, which, for all points in the scan, is at least 30 times the electron-neutral collision frequency. The ion gyrofrequency is $\sim 4 \times 10^5$ rad/s, while the ion-neutral collision frequency varies from $4 - 35 \times 10^5$ Hz.

The electron mean free path, calculated using the classical formula [18] for electron-ion collisions, and tabulated electron-neutral momentum transfer cross sections [19], is shown in Fig. 2c. The values are scaled to the current sheet half-width, δ_{CS}. At low values of ρ/ρ_i, the electrons are marginally collisionless, and any collisions that due occur are with ions. As the neutral density increases, the electrons become fully collisional. However, unlike previous studies of two-fluid effects [20], this is due to collisions with neutrals and not ions. This may seem contradictory as fast Hall reconnection is often referred to as "collisionless" reconnection. This can be resolved by noting that fully ionized collisional plasmas tend to have short ion inertial lengths due to high densities, but this is not necessarily the case for weakly ionized plasmas.

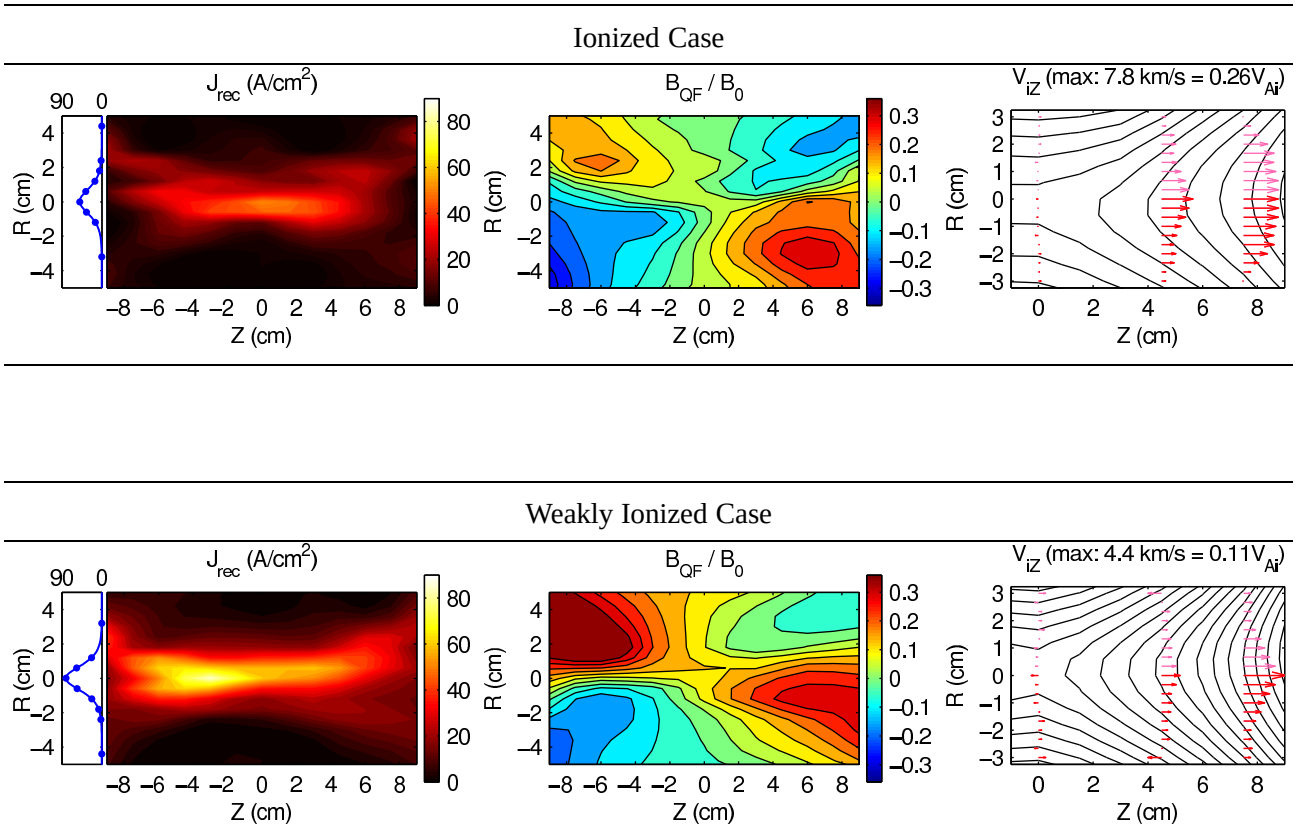

FIG. 3. (color). For each ionization case: (left) Reconnection current sheet density. (middle) Out-of-plane magnetic field, scaled to the upstream field. (right) Z component of the ion flow velocity with magnetic flux contours. Red arrows are actual measurements, pink arrows are reflections about $R = 0$ to guide the eye.

In Fig. 2d, we show the ion outflow time scaled to the ion-neutral collision frequency, $L\nu_{in}/v_{Ai}$, where L is the current sheet half-length and He charge-exchange cross sections [21] were used. Again, at low values of ρ/ρ_i, the outflow ions are only marginally coupled with the neutrals, but become increasingly collisional as the neutral density increases. However, since δ_{CS} is a much shorter scale length, they are not coupled in the inflow except in the highest ρ/ρ_i cases.

We now consider the two extreme cases in the scan in detail. At $\rho/\rho_i \sim 8$, electrons collide primarily with ions, and ions and neutrals are only moderately coupled ($\lambda_{in} \gg \delta_{CS}, \sim L_{CS}$), so we consider this to be the "ionized case." At the other end of the scan, $\rho/\rho_i \sim 70$, both electron and ions are strongly collisional with neutrals, so we consider this to be the "weakly ionized case."

In the left column of Fig. 3, we show the reconnection current sheet density for each of these cases. The line cuts show the Harris function fit [22, 23] at $Z = 0$ cm, which shows δ_{CS} for each case. The current sheet dimensions are similar, although the magnitude of the current is larger in the weakly ionized case. This is reminiscent of previous models [24, 25] that showed that

ambipolar diffusion (ion-neutral drift) can steepen the B profile to form stronger current sheets. It should be noted that the Hall term was not included in their models, but plays a significant role here, so the comparison is only qualitative. The combination of these effects will be investigated in a future work.

In the middle column, we plot the out-of-plane quadrupole field (QF), which is a signature of Hall reconnection [26, 27], scaled to the upstream reconnecting field. In both cases the structure and scaled magnitude of the QF are similar. The scale size of the QF, taken to be the Z displacement between the peaks of the lobes, is approximately 5 cm or 0.5 δ_i, where δ_i is the ion inertial length. This is consistent with previous results in ionized plasmas [28], although somewhat surprising since we expect the enhanced effective ion mass to broaden this scale by a factor of $\sqrt{\rho/\rho_i}$ [11].

Another indicator of the ion layer scale can be found by looking at the detailed structure of the ion outflow region. The outflow region of half of the reconnection layer is shown in the right column of Fig. 3 for each of the ionization cases. As described earlier, radial profiles can be measured in a single shot by translating the reconnection layer past one stationary Mach probe. Only one probe was used for this dataset, so different Z locations are measured by taking multiple shots (with the same experimental parameters) and with the probe in different locations. The scale size of the outflow channel, measured as the width in the R direction of flow profile, is about the same for each case.

Note however, that the magnitude of the outflow is greatly reduced in the weakly ionized case. Even at the highest ionization fraction achieved in this scan, there is some coupling in the outflow direction since $L_{CS} \sim 2.8\lambda_{in}$, where L_{CS} is the current sheet half-length. The effect of this coupling can be seen in Fig. 4, which shows the ion outflow speed at $Z = 7.5$ cm $(\sim L_{CS})$ for each value of ρ/ρ_i. The outflow speed, when normalized to the plasma Alfvén speed (blue squares), decreases according to $\sqrt{\rho/\rho_i}$, which shows that the outflow speed is actually limited to the bulk Alfvén velocity. When normalized to this value, the outflows are all approximately 1, shown by red circles in Fig. 4.

In a previous experiment on MRX, Ji *et al.* [29] found that plasma pileup and compressibility were also found to significantly reduce the outflow speed in MRX. In this parameter regime, where the plasma density is lower and flows are mostly subsonic, these effects do not play such an important role. If we account for these effects, then the outflow speeds are predicted to be $\sim 0.8 v_{Ai}$ for the ionized cases, and nearly Alfvénic for the weakly ionized cases. Since the observed outflows

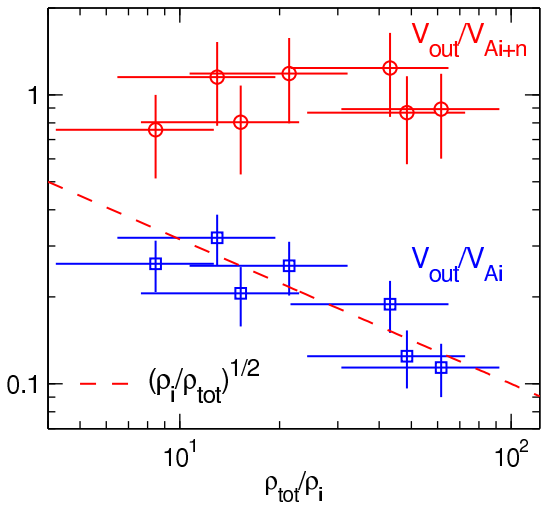

FIG. 4. (color online). Average reconnection ion outflow speed at $Z = 7.5$ cm, scaled as a function of neutral density ratio. Blue squares are scaled to the plasma Alfvén speed, and dashed red line shows $(\rho_i/\rho)^{1/2}$ scaling. Red circles show the outflow scaled to the bulk Alfvén speed.

are much slower, and scale as expected with ρ/ρ_i, we conclude that ion-neutral drag is most likely to be responsible for most or all of the outflow reduction. Note that differences in neutral pressure, which have not been yet measured, may also be playing a role, and will be investigated in a future work.

Finally, we return the full scan to discuss the reconnection rate. In Fig. 5a, we show the reconnection electric field, normalized to the *plasma* Alfvén speed, V_{Ai} and upstream magnetic field. With this normalization, the reconnection rate steadily decreases as neutrals are added. A model for Hall reconnection in partially ionized plasmas [11] has predicted that this rate should be independent of ρ/ρ_i. This occurs because, while the outflow is slowed by a factor of $\sqrt{\rho/\rho_i}$, the ion layer scale size expands by the same factor. Therefore the total ion flux is the same, and so is the reconnection rate. As described above, we observe the outflow reduction, but not the layer expansion. Indeed, if we normalize E to the bulk Alfvén velocity (red circles in Fig. 5a), then the reconnection rate is constant. Note that a Sweet-Parker analysis with neutral drag added predicts a reduction that goes like $(\rho/\rho_i)^{1/4}$, which is not as severe as the observed reduction.

It is interesting to note that $E/(B_0 V_{Ai+n})$ is about unity for all of these cases. For steady state reconnection, this indicates that the aspect ratio of the ion layer is also of order unity. One possible explanation for this result is system size and boundary effects. Malyshkin and Zweibel [11] assumed that the system size is large enough to accomodate the scale expansion caused by

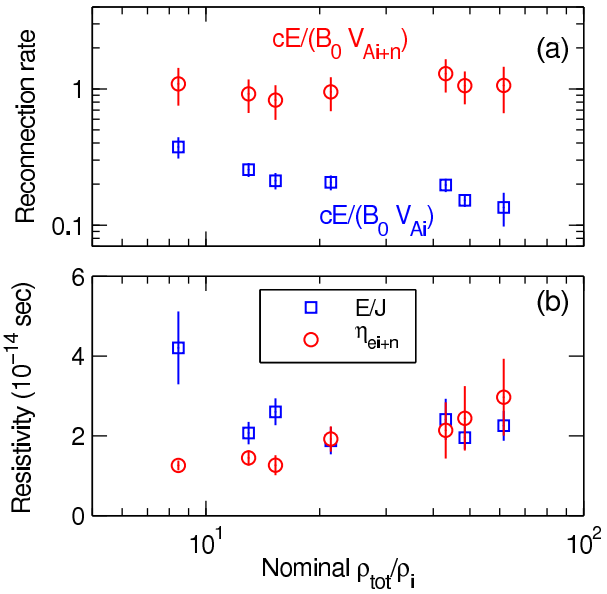

FIG. 5. (color online). As a function of nominal neutral density ratio: (a) reconnection rate normalized to the plasma and bulk Alfvén speeds; (b) measured effective resistivity (E/J) at the X-point, and classical resistivity due to electron collisions with ions and neutrals.

the increased effective ion mass. In this experiment, at $\rho/\rho_i \sim 70$, the predicted effective ion inertial length is 83 cm, which is larger than the current MRX system size, so the ion layer may not be able to expand as predicted by the boundary-free theory, and is restricted to a unity aspect ratio layer. This could be studied further by including boundary effects in the theory, using future reconnection experiments [30], or through simulations capable of including multi-fluid effects.

The calculated classical resistivity [18] due to electron collisions with both ions and neutrals, η_{ei+n} is shown as red circles in Fig. 5b. The effective resistivity (E/J at the X-point, blue squares) is higher than the classical value for conditions where the electrons are not collisional, presumably due to anomalous resistivity and consistent with previous results [29]. It then agrees with the classical value as electron collisionality increases (compare Fig. 2c). Note that the resistivity levels off/increases at high ρ/ρ_i, while the reconnection rate continues to decrease. This is further evidence that the rate is set by ion dynamics, and is not strongly dependent on the dissipation mechanism.

In summary, we have demonstrated that fast Hall reconnection can occur in a weakly ionized plasma. Ion-neutral drag reduces the ion outflow speed by a factor of $\sqrt{\rho/\rho_i}$. However, in contrast with theoretical predictions, the transverse scale of the outflow channel does not expand by the same factor, and therefore the ion-controlled reconnection rate is reduced.

We thank L. Malyshkin and E. Zweibel for many useful discussions, and R. Cutler and P. Sloboda for providing technical expertise. This work was supported by the US Department of Energy.

[1] N. Nishizuka, M. Shimizu, T. Nakamura, K. Otsuji, T. Okamoto, Y. Katsukawa, and K. Shibata, The Astrophysical Journal Letters **683**, L83 (2008).

[2] B. De Pontieu, S. W. McIntosh, V. H. Hansteen, and C. J. Schrijver, The Astrophysical Journal Letters **701**, L1 (2009).

[3] T. Cowling, *Magnetohydrodynamics* (Interscience, 1957).

[4] L. Mestel and L. Spitzer, Jr., Mon. Not. Roy. Astron. Soc. **116**, 503 (1956).

[5] E. G. Zweibel, Astrophys. J. **340**, 550 (1989).

[6] S. Takasao, A. Asai, H. Isobe, and K. Shibata, The Astrophysical Journal Letters **745**, L6 (2012).

[7] S. I. Syrovatskii, Annual Review of Astronomy and Astrophysics **19**, 163 (1981).

[8] D. Biskamp, Physics of Fluids **29**, 1520 (1986).

[9] Lockheed-Martin Solar & Astrophysics Laboratory, "IRIS Project Page," `http://science.nasa.gov/missions/iris/` (2012).

[10] D. G. Swanson, R. W. Gould, and R. H. Hertel, Phys. Fluids **7**, 269 (1964).

[11] L. M. Malyshkin and E. G. Zweibel, Astrophys. J. **739**, 72 (2011).

[12] E. G. Zweibel, E. Lawrence, J. Yoo, H. Ji, M. Yamada, and L. M. Malyshkin, Physics of Plasmas **18**, 111211 (2011).

[13] D. Biskamp, E. Schwarz, and J. F. Drake, Phys. Rev. Lett. **75**, 3850 (1995).

[14] M. Yamada, H. Ji, S. C. Hsu, T. Carter, R. M. Kulsrud, N. Bretz, F. Jobes, Y. Ono, and F. Perkins, Phys. Plasmas **4**, 1936 (1997).

[15] I. H. Hutchinson, *Principles of Plasma Diagnostics* (Cambridge University Press, 2005).

[16] M. Yamada, J. Yoo, T. Tharp, H. Ji, and E. Lawrence, Bull. Am. Phys. Soc. **53**, 9057P (2011).

[17] D. Stotler, D. Post, and D. Reiter, Bull. Am. Phys. Soc. **38**, 1919 (1993).

[18] S. Braginskii, in *Rev. Plasma Phys.*, Vol. 1 (Consultants Bureau, New York, 1965) pp. 201–311.

[19] Y. Itikawa, At. Data Nucl. Data Tables **21**, 69 (1978).

[20] M. Yamada, Y. Ren, H. Ji, J. Breslau, S. Gerhardt, R. Kulsrud, and A. Kuritsyn, Phys. Plasmas **13**, 052119 (2006).

[21] R. K. Janev, W. Langer, K. Evans, and D. E. Post, *Elementary Processes in Hydrogen-Helium Plasmas* (Springer-Verlag, 1987).

[22] E. Harris, Il Nuovu Cimento **23**, 115 (1962).

[23] M. Yamada, H. Ji, S. Hsu, T. Carter, R. Kulsrud, and F. Trintchouk, Phys. Plasmas **7**, 1781 (2000).

[24] A. Brandenburg and E. G. Zweibel, Astrophysical Journal (1994).

[25] F. Heitsch and E. G. Zweibel, Astrophys. J. **583**, 229 (2003).

[26] M. Mandt, R. Denton, and J. Drake, Geophys. Res. Lett. **21**, 73 (1994).

[27] M. Shay, J. Drake, R. Denton, and D. Biskamp, J. Geophys. Res. **103**, 9165 (1998).

[28] Y. Ren, M. Yamada, H. Ji, S. Dorfman, S. Gerhardt, and R. Kulsrud, Phys. Plasmas **15**, 082113 (2008).

[29] H. Ji, M. Yamada, S. Hsu, and R. Kulsrud, Phys. Rev. Lett **80**, 3256 (1998).

[30] H. Ji and W. Daughton, Phys. Plasmas **18**, 111207 (2011).